PCCP

PAPER

Cite this: *Phys. Chem. Chem. Phys.*, 2019, **21**, 3669

The Gigahertz and Terahertz spectrum of monodeutero-oxirane (c-C_2H_3DO)†

Sieghard Albert,[a] Ziqiu Chen,[ab] Karen Keppler,[a] Philippe Lerch,[c] Martin Quack,*[a] Volker Schurig[d] and Oliver Trapp[e]

Received 20th August 2018,
Accepted 24th October 2018

DOI: 10.1039/c8cp05311a

rsc.li/pccp

The rotational spectrum of monodeutero-oxirane was analysed as measured using the Zurich Gigahertz (GHz) spectrometer and our highest resolution Fourier Transform Infrared (FTIR) spectrometer system coupled to synchrotron radiation at the Swiss Light Source (SLS). 112 distinct line frequencies have been newly assigned in the GHz range (extended to 120 GHz, compared to previous work extending to only 59 GHz) including rotational states up to J = 23. We have furthermore assigned 398 lines in the far infrared or Terahertz range (0.75–2.10 THz or 25–70 cm^{-1}) including transitions with rotational quantum numbers up to J = 59. The results are discussed in relation to the possible first astrophysical observation of an isotopically chiral molecule and in relation to molecular parity violation.

1. Introduction

Deuterated molecules have been detected in several interstellar objects.[1,2] Interestingly, the D/H ratio for some of the interstellar molecules is much higher than the galactic value. An interesting candidate for astrophysical observation to help further understanding of this effect is monodeutero-oxirane (c-C_2H_3DO) because this molecule is isotopically chiral[3–5] (Fig. 1 shows the absolute configurations of the enantiomers of c-C_2H_3DO). The undeuterated parent species, oxirane or ethylene oxide (c-C_2H_4O), is a small cyclic molecule. Oxirane is an isomer of acetaldehyde (CH_3CHO), which is more stable by about 1 eV or 100 kJ mol^{-1}. Oxirane is kinetically stable at ordinary temperatures in the laboratory. Oxirane was first detected in Sgr B2N[6] and then in several other hot-core sources,[7] several other environments[8] and the central molecular zone in our galactic center.[9] It might be also a candidate as a carrier of some unidentified infrared bands.[10] The relatively high abundance of oxirane in interstellar space indicates that monodeutero-oxirane may become the first isotopically chiral molecule to be detected by astrophysical observations.

The rotational constants of the vibrational ground state of oxirane in the electronic ground state ($^1A_1$ in C_{2v}) have been determined by microwave spectroscopy,[11–13] submillimeter spectroscopy[14] using the FASSST system[15] and recently by synchrotron-based THz spectroscopy.[16] The rovibrationally resolved infrared spectrum of oxirane has also been analysed in the range 600 to 3500 cm^{-1}.[17–21] Although the parent oxirane has been studied extensively in the spectroscopic investigations mentioned, monodeutero-oxirane has received little attention by comparison. The only microwave study, approximately 40 years ago, assigned 20 pure rotational transitions.[12] Recently, calculated spectroscopic parameters including rotational constants and centrifugal distortion constants up to sextic terms have been provided.[22] High resolution FTIR spectroscopic analyses of this type of molecule have been available for the closely related

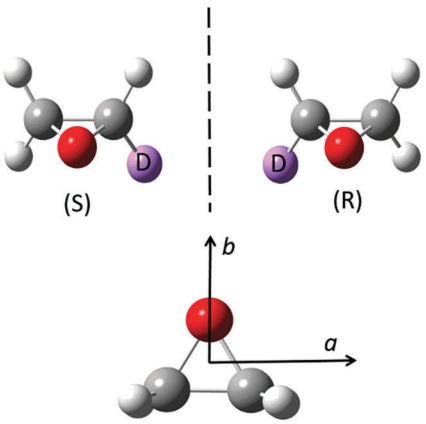

Fig. 1 Structures of the (*S*)- and (*R*) monodeutero-oxirane (top, carbon atoms are labelled in grey, hydrogen light grey, oxygen red and deuterium violet). Axes definition in the principal inertial axis system is shown at the bottom. The *c*(*z*)-axis is perpendicular to the *a*(*x*)*b*(*y*) plane pointing toward the observer.

[a] *Physical Chemistry, ETH Zürich, CH-8093 Zürich, Switzerland. E-mail: martin@quack.ch; Fax: +41-44-632-1021; Tel: +41-44-632-4421*
[b] *College of Chemistry and Chemical Engineering, Lanzhou University, Lanzhou 730000, China*
[c] *Swiss Light Source, Paul Scherrer Institute, CH-5232 Villigen, Switzerland*
[d] *Institute of Organic Chemistry, University of Tubingen, Tubingen, Germany*
[e] *Department of Chemistry, Ludwig Maximilians University, Munich, Germany*

† Electronic supplementary information (ESI) available: Linelists of transitions assigned are included. See DOI: 10.1039/c8cp05311a

chiral fluorooxirane,[23] which is a candidate for the study of molecular parity violation.[24]

The current study aims to significantly extend the range of laboratory spectroscopy to support the astrophysical observation of monodeutero-oxirane by a combined GHz and THz analysis of its pure rotational spectrum. We report the measurement and analysis of the observed spectra of C_2H_3DO in the vibrational ground state in the ranges of 62 to 120 GHz and 25 to 70 cm^{-1} (0.75–2.10 THz). Some preliminary results of the present project were reported in ref. 25–27.

2. Experimental

2.1 Sample of monodeutero-oxirane

The synthesis has been reported in ref. 25 in more detail. In brief, in a protective atmosphere, vinyl magnesium chloride solution in THF was quenched with deuterium oxide and monodeuteroethene was introduced into a freshly prepared solution of acetylhypobromide (from silver acetate and bromine) in anhydrous tetrachloromethane. After completion of the reaction, the solution was washed with 10% sodium hydrogen sulphate, and dried over magnesium sulphate. The solvent was removed. The crude product (1-acetoxy-2-bromo[^{2}H]ethane) was distilled under vacuum (60 °C at 30 Torr). 1-Acetoxy-2-bromo[^{2}H]ethane and 25% sodium hydroxide in solution were combined in a flask equipped with a condenser filled with a molecular sieve (3 Å) and a nitrogen gas inlet. The flask was heated to 100 °C and monodeutero-oxirane was condensed in a cryogenic trap. The product was redistilled at 10.7 °C. The product was identified by NMR and mass spectrometry and the identity and purity were also obvious from the GHz and THz spectra, which also showed some methylene chloride CH_2Cl_2 present as an impurity, which could be clearly identified and thus does not negatively affect the analysis.

2.2 GHz measurements

The rotational spectra of monodeutero-oxirane in the GHz region were measured using our Zurich GHz spectrometer described in detail recently.[28,29] It consists of an Agilent synthesizer (E8257D PSG, Agilent Technologies Option 520 UNX) working in the range 250 kHz to 20 GHz with a frequency resolution of 0.001 Hz and frequency locked to a 10 MHz-rubidium standard (FS725, Stanford Research Systems) for short-term stability and to a GPS standard (TM-4, Spectrum Instruments Inc.) for long-term stability leading to a frequency uncertainty of only $\Delta\nu/\nu = 10^{-11}$. The signal is frequency multiplied by a factor of 6 (S10MS-AG, OML Inc.) and coupled out to free space *via* a conical W-band antenna (QWH-WCRR, QuinStar Technology Inc.) leading to an operation in the frequency range of 67 to 118 GHz. The beam is focused through Teflon lenses into a 2.5 m cell equipped with two Teflon windows and mounted in a Brewster angle to the incoming and outcoming beam. Finally, the beam is detected using a two-channel indium antimonide (InSb) bolometer [QFI/2(2), QMC Instruments Ltd] after passing a second Teflon lens. All transitions were collected using the frequency modulation technique (second harmonic lock-in detection) with a modulation frequency of 50 kHz. The final combined uncertainty in the line frequencies is estimated to be about 200 kHz.

The high sensitivity of this setup has been demonstrated in our recent high resolution spectroscopic studies of 1,2-dithiine[29,30] and deuterated phenols.[31] The survey spectra were recorded first between 69 and 113 GHz in 3 GHz segments at p = 25 μbar, followed by subsequent close examinations of each individual line by choosing a narrow bandwidth ($\sim$5 MHz) with longer integration time for the best signal-to-noise (S/N) ratios. This procedure allowed for measurements of weaker transitions. Eventually, with better predictions based on an improved effective Hamiltonian, the measurement of individual lines was extended to 62 GHz (lower limit) and 120 GHz (upper limit).

2.3 THz measurements (FTIR spectra)

Although the Far-IR/THz region is traditionally difficult for FTIR spectroscopy, the IR-beamline at the synchrotron facility of Switzerland (Swiss Light Source – SLS) has proved to produce an advantage of up to a factor of 50 over traditional Hg-lamp sources in terms of S/N ratios,[32] making it possible to probe pure rotational levels of monodeutero-oxirane. The ETH-SLS Bruker IFS 125 HR prototype 2009 spectrometer was used to record the spectra in the THz range: this spectrometer provides the highest resolution currently available by FTIR spectroscopy worldwide, corresponding to a maximum optical path difference of d_{MOPD} = 11.7 m and an effective resolution of better than 0.0006 cm^{-1}.[29–35]

The spectrometer is connected *via* transfer optics to the switchyard of the infrared port at the SLS, consisting of one parabolic, two toroidal and one flat mirror. The toroidal mirrors are necessary due to the strong astigmatism of the synchrotron beam. It has the shape of a curved 3D filament. A parallel beam entering the source chamber of the spectrometer is focused onto the aperture using a parabolic mirror with focal length 41.8 cm, yielding a diameter as small as 0.5 mm, and passes on into the interferometer. The Maximum Optical Path Differences (MOPD) of d_{MOPD} = 11.7 m leads to a best possible unapodized instrumental bandwidth of 0.00052 cm^{-1} or 16 MHz (Full-Width at Half-Maximum, FWHM). This spectrometer is a further development of our IFS 120/125 Prototype 2001.[32,34,35] The rotational spectra in the range 25 to 70 cm^{-1} (0.75–2.10 THz) were recorded with the maximum d_{MOPD} of 11.7 m. A 6 μm Mylar beamsplitter, an aperture of 3.15 mm and a liquid He-cooled bolometer were used for the measurements. The scanner velocity (modulation frequency) was 30 kHz. Several spectra with pressures between 0.3 and 10 mbar have been recorded. Fig. 2 shows an overview of the measured THz spectra of monodeutero-oxirane. All wavenumbers were calibrated with residual H_2O vapor lines between 50 and 90 cm^{-1} as compared to values reported in the HITRAN database.[36] Of course, neither the H_2O impurity lines nor the other impurity lines (CH_2Cl_2) have any negative effects on the high resolution analysis of the monodeutero-oxirane spectrum, which was unambiguously assigned. As only a small

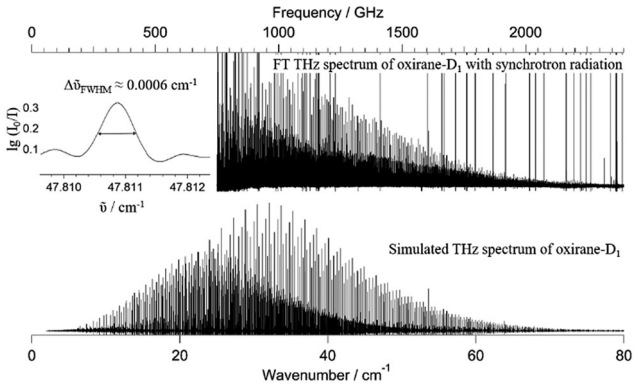

Fig. 2 An overview of the THz spectrum of C_2H_3DO between 0.75 and 2.5 THz. Decadic absorbance $\lg(I_0/I)$ is shown where the cutoff at maximum absorbance has the value of 2, pathlength l = 10 m, pressure = 0.8 mbar and temperature T = 295 K. The insert in the top-left corner shows an example of the typical line with full-width at half-maximum of about 0.0006 cm^{-1} in the measured range.

and precious sample was available for this isotopomer, we decided against any attempts of further purification, which was not necessary for our analysis and would have jeopardized the sample.

In general, wavenumbers measured in this spectral range are estimated to be accurate to within about 0.0001 cm^{-1}. The data given in the line lists of the ESI† correspond to calibrated line maxima. The insert in Fig. 2 shows a typical linewidth (FWHM) of 0.0006 cm^{-1}. The Doppler width is about 0.00009 cm^{-1} at 50 cm^{-1}, indicating that the resolution is instrument limited. The measured line widths indicate the absence of significant pressure broadening in agreement with expected widths from pressure broadening (less than about 10^{-4} cm^{-1} for the conditions of Fig. 2).

3. Assignment and analysis

3.1 Effective Hamiltonian

The analyses of the rotational spectra in the GHz and THz regions were carried out using Watson's A-reduced effective Hamiltonian[37] in the I^r representation, which is used here including up to sextic centrifugal distortion constants:

$$\begin{aligned}\hat{H}^{v,v}_{rot} &= A_v\hat{J}_z^2 + B_v\hat{J}_x^2 + C_v\hat{J}_y^2 \\ &\quad - \Delta_J^v\hat{J}^4 - \Delta_{JK}^v\hat{J}^2\hat{J}_z^2 + \Delta_K^v\hat{J}_z^4 \\ &\quad - \frac{1}{2}\left[\left(\delta_J^v\hat{J}^2 + \delta_K^v\hat{J}_z^2\right), \left(\hat{J}_+^2 + \hat{J}_-^2\right)\right]_+ \\ &\quad + \phi_J^v\hat{J}^6 + \phi_{JK}^v\hat{J}^4\hat{J}_z^2 + \phi_{KJ}^v\hat{J}^2\hat{J}_z^4 + \phi_K^v\hat{J}_z^6 \\ &\quad + \frac{1}{2}\left[\left(\eta_J^v\hat{J}^4 + \eta_{JK}^v\hat{J}^2\hat{J}_z^2 + \eta_K^v\hat{J}_z^4\right), \left(\hat{J}_+^2 + \hat{J}_-^2\right)\right]_+\end{aligned}$$

where with $i = \sqrt{-1}$ we have the angular momentum operators:

$$\hat{J}^2 = \hat{J}_x^2 + \hat{J}_y^2 + \hat{J}_z^2, \quad \hat{J}_\pm = \hat{J}_x \pm i\hat{J}_y$$

The analyses and fits used the WANG program.[38,39]

3.2 Assignment of the pure rotational spectra in the ground state

As a three-membered heterocyclic molecule, the heavy atom skeleton of the ground state structure of monodeutero-oxirane is co-planar. Based on an early microwave study of C_2H_4O by Gwinn and co-workers, which showed one electric dipole moment component in the molecular plane $\mu_b = 1.88 \pm 0.01$ D using Stark effect measurements,[11] we expect a similar μ_b in C_2H_3DO and the components μ_a and μ_c due to the deuterium substitution to be nonzero but quite small in absolute value (see, for instance, CH_3D,[40] CD_3H[41] and CH_2D_2[42] for comparison). The principal axis system for C_2H_3DO is given in Fig. 1.

The assignment of the GHz spectra was assisted by the previously reported rotational constants in ref. 12, which were based on the analysis of 20 transitions with $J_{max} = 8$ and $K_{c,max} = 4$. 112 distinct lines obeying b-type selection rules for K_aK_c quantum numbers (oe ↔ eo and ee ↔ oo)[43,44] were assigned using the PGOPHER program[45,46] in the range of 62–120 GHz with $J_{max} = 23$ and $K_{c,max} = 14$. The newly assigned transitions were fitted separately and the resulting rotational parameters are given in Table 1. The root-mean-square deviation d_{rms} of the fit is less than 30 kHz, with the typical linewidths (FWHM) being about 200 kHz. The rotational constants agree with those obtained previously using microwave spectroscopy.[12] The centrifugal distortion constants are determined here for the first time. Subsequently, this enlarged set of improved spectroscopic parameters led to a reasonably good prediction for the pure rotational spectra with higher J value transitions in the THz region. After further transitions were added to the assigned line list of the GHz spectra and fitted, the simulated spectrum was refined leading to the assignment of more transitions. This iterative process continued until all the stronger transitions had been accounted for. An additional 398 distinct lines were assigned between 0.75 and 2.10 THz (25 to 70 cm^{-1}) and co-fitted with transitions assigned in the GHz region as well as MW lines reported by ref. 12. The resulting spectroscopic parameters of the global fit are presented in Table 2.

4. Discussion

The assignment and analysis of the pure rotational spectra measured in the GHz region over a range of ~58 GHz provide a

Table 1 Spectroscopic parameters for the ground state of monodeutero-oxirane from the MW and GHz spectra in MHz (values in parentheses provide statistical 1σ uncertainties in units of the last specified digits)

	MW previous (ref. 12)	GHz this work
A/MHz	24252.47(17)	24252.64843(23)
B/MHz	19905.34(17)	19905.52198(19)
C/MHz	13327.40(17)	13327.58408(16)
Δ_J/kHz	—	17.01001(37)
Δ_K/kHz	—	25.44301(72)
Δ_{JK}/kHz	—	17.31528(86)
δ_j/kHz	—	13.17077(19)
δ_k/kHz	—	4.74440(16)
d_{rms}/kHz	—	30
N	20	112

Table 2 Spectroscopic parameters in cm^{-1} for the ground state of C_2H_3DO (Tables S1 and S2 are available as part of the ESI)[a]

	Only MW and GHz corresponding to Table S1 (ESI)	MW, GHz and THz combined corresponding to Table S2 (ESI)	Theory CCSD(T)/ cc-pVTZ scaled[b]
A/cm^{-1}	0.808981247	0.808981247	0.8089040
B/cm^{-1}	0.663976719	0.663976719	0.6640071
C/cm^{-1}	0.444560261	0.444560261	0.4445481
$\Delta_J/10^{-6}$ cm^{-1}	0.5715(84)	0.56954(23)	0.52333
$\Delta_K/10^{-6}$ cm^{-1}	0.8468(15)	0.84986(69)	0.58233
$\Delta_{JK}/10^{-6}$ cm^{-1}	0.5798(17)	0.57548(72)	0.74725
$\delta_J/10^{-6}$ cm^{-1}	0.15857(21)	0.158105(69)	0.1376
$\delta_K/10^{-6}$ cm^{-1}	0.4382(11)	0.44198(35)	0.54084
$\phi_J/10^{-12}$ cm^{-1}	—	0.47(7)	0.20
$\phi_{JK}/10^{-12}$ cm^{-1}	—	6.2(7)	5.681
$\phi_{KJ}/10^{-12}$ cm^{-1}	—	−32(2)	−28.98
$\phi_K/10^{-12}$ cm^{-1}	—	29(2)	25.27
$\eta_J/10^{-12}$ cm^{-1}	—	0.063[c]	0.063
$\eta_{JK}/10^{-12}$ cm^{-1}	—	2.71[c]	2.71
$\eta_K/10^{-12}$ cm^{-1}	—	2.06[c]	2.06
d_{rms}/cm^{-1}	0.0000035	0.000079	
N	132	530	

[a] Values in parentheses indicate uncertainties as 1σ in units of the last digits given. Rotational constants without parenthesis were held fixed at the values of the ground state obtained by fitting only transitions in the MW and GHz region. [b] Values from ref. 22. [c] Fixed at the *ab initio* estimate from ref. 22.

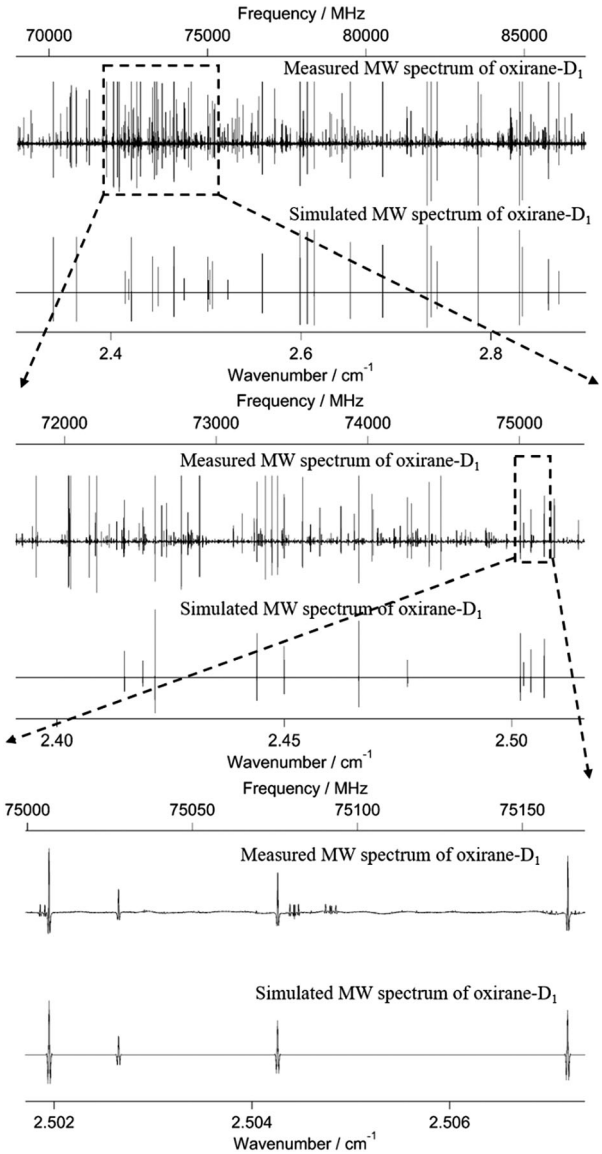

Fig. 3 A comparison of observed and simulated rotational spectra of C_2H_3DO in the GHz region. The unassigned lines exhibit hyperfine splitting patterns presumably due to nuclear quadrupole moment couplings in the impurity CH_2Cl_2 (unresolved in oxirane-D1). The unassigned line frequencies are as expected for $CH_2{}^{35}Cl_2$.[47]

much broader coverage of energy levels than the earlier microwave study.[12] This allowed for a new and accurate determination of centrifugal distortion constants of the ground state of monodeutero-oxirane, not available previously, in addition to more accurate rotational constants. The small $d_{rms} \approx 30$ kHz of the fit using only three rotational constants and five centrifugal distortion constants suggests that the effective Hamiltonian employed here provides an accurate description of the observed spectra in this range. This success in modelling is evident in the comparison between experimental and simulated GHz spectra shown in Fig. 3 using the spectroscopic parameters in Table 1. Fig. 4 shows a comparison of simulations based on the early microwave work[12] and our new analysis. Clearly, the prediction based on a model Hamiltonian with only three rotational constants cannot be extrapolated to guide field observations beyond the measurement range. In this case, the extended spectral range was vital in providing more accurate predictions of line frequencies, especially those with high J and K_c values which are more sensitive to centrifugal distortion constants.

For the assignment of the THz spectra, which consist of transitions with higher J and K_c values, additional higher order centrifugal constants up to the sextic terms were used for the convergence of the fit. The global fit of combined MHz, GHz and THz transitions has a d_{rms} of only 0.000079 cm^{-1} ($\sim$2 MHz). This small d_{rms} is yet another illustration of the excellent agreement between the observed spectra and the effective Hamiltonian employed. A comparison of the experimental THz spectra and the simulation based on spectroscopic parameters reported in Table 2 is presented in Fig. 5. Although most simulated spectral lines, if not all, are accounted for in both the GHz and THz spectra, as shown in Fig. 3 and 5, it can be seen that a few lines still remain unassigned, especially in the THz range. We first noticed these extra lines in the GHz spectra, where clusters of lines with different linewidths are present. The patterns look like hyperfine splittings from nuclear quadrupole couplings which are expected to be negligible in C_2H_3DO at this resolution. Fig. 3 shows an example of such line structures. Furthermore, Fig. 6 shows that the simulated spectra of methylene chloride ($CH_2{}^{35}Cl_2$) match many unassigned lines in the experimental THz spectra well. Thus, we concluded that these extra lines are due to contaminants including at least dichloromethane, and have no spectroscopic implications other than causing spectral overlapping and, in some cases, congestion. Interestingly, having impurities in our experimental sample has

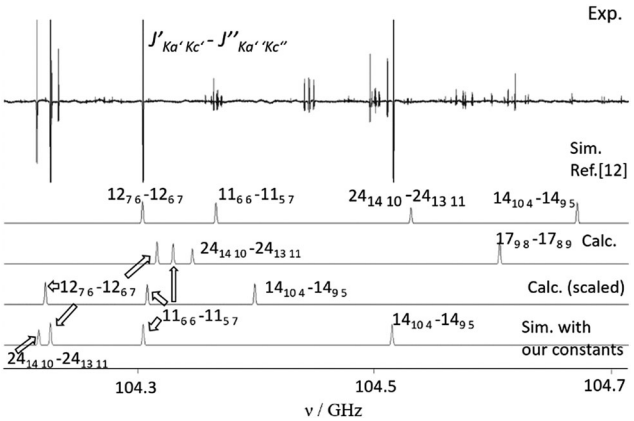

Fig. 4 A comparison of the GHz spectrum of C_2H_3DO (from top to bottom): (1) observed spectrum; (2) simulated spectrum based on early MW work in ref. 12; (3) calculated (unscaled) spectrum (CCSD(T)/cc-pVTZ) in ref. 22; (4) calculated (scaled) spectrum (CCSD(T)/cc-pVTZ) in ref. 22; (5) simulated spectrum with our constants. The quantum numbers of the transitions are arranged in the form of $J_{K_a' K_c'}' - J_{K_a'' K_c''}''$.

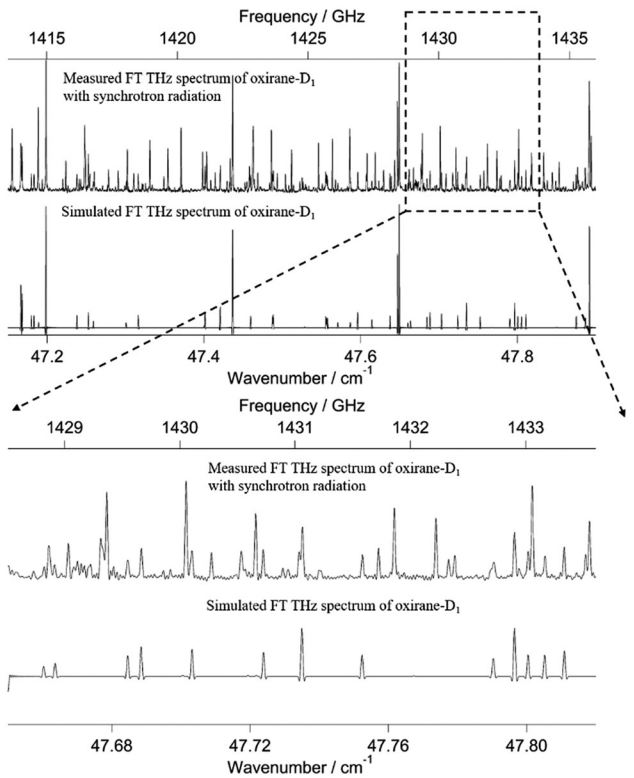

Fig. 5 A comparison of observed and simulated rotational spectra of C_2H_3DO in the THz region. Decadic absorbance $\lg(I_0/I)$ is shown where the cut-off at maximum absorbance has the value of 0.9, pathlength l = 10 m, pressure = 0.8 mbar and temperature = 295 K.

demonstrated the power of high resolution spectroscopy in providing unambiguous identification of molecules in a mixture, which is the cornerstone of remote sensing.

The recent *ab initio* calculation by Puzzarini *et al.*[22] provided ground state spectroscopic parameters at the CCSD(T)/cc-pVTZ level. In general, the calculated parameters are close to experimental

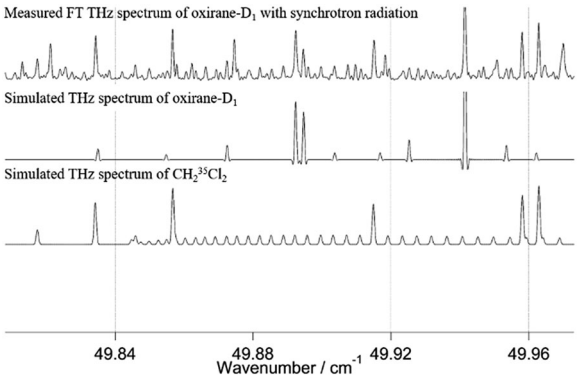

Fig. 6 A comparison of (from top to bottom): (1) observed THz spectrum; (2) simulated C_2H_3DO spectrum; (3) simulated $CH_2{}^{35}Cl_2$ spectrum. Decadic absorbance $\lg(I_0/I)$ is shown where the cut-off at maximum absorbance has the value of 0.55, pathlength l = 10 m, pressure = 0.8 mbar and temperature = 295 K.

values determined here (see Table 2). In fact, the rotational constants were calculated with a relative deviation of less than 0.15%. This small uncertainty is, indeed, an excellent achievement in terms of *ab initio* theory by experts in the field. However, it would not be sufficient in spectroscopy at high resolution when it comes to a desired "line-by-line" assignment in searches in the field, in which the signal of molecules of interest is often mixed with the signal associated with other components of the mixture being examined. Fig. 4 shows that not only are the transitions shifted by about 100 MHz at 104 GHz but in addition, the simulated spectrum also failed to reproduce the rotational structure of C_2H_3DO, upon which field assignments strongly rely. This would add ambiguity to the assignment effort, particularly when congested, complicated spectra are being examined. Puzzarini *et al.* in ref. 22 further scaled the calculated parameters using the theoretical best estimate and experimental data for the main isotope. The scaling factor improved the calculation considerably and this can be seen in Fig. 4: two strong lines $12_{7\,6}$–$12_{6\,7}$ and $11_{6\,6}$–$11_{5\,7}$ are within 5 MHz of the predictions, however, transitions with higher K_a values are still off by more than 100 MHz. On the other hand, the fact that the scaling factor obtained from the normal oxirane works reasonably well on the mono-deuterated species is hardly surprising, because this highly strained three-membered heterocycle is expected to be rigid (as opposed to non-rigid in the sense of Longuet–Higgins[3,51]) and the deuterium substitution leads to a minor change of rotational constants only.

5. Conclusions

Our work has substantially extended the high resolution rotational spectroscopy of monodeutero-oxirane in the GHz region. The brightness of the synchrotron radiation made it possible to record and analyse, for the first time, pure rotational spectra of monodeutero-oxirane (C_2H_3DO) in the THz region, in which traditional FTIR spectroscopy has difficulty acquiring high quality data. The spectroscopic analyses of the combined GHz and THz spectra resulted in a model Hamiltonian which

accurately determines the centrifugal distortion constants, not available previously. This new set of spectroscopic parameters is essential for predicting suitable transitions for astronomical observations in the interstellar medium up to and beyond the frequencies reported here. A very recent publication reported the first detection of oxirane (C_2H_4O) in the low-mass protostar IRAS 163–2422 using the Atacama Large Millimeter/submillimeter Array (ALMA).[48] As this detection was made in the range between 329 GHz and 362 GHz, which lies between the two regions covered by our work, the prediction of lines with the effective Hamiltonian of the present work should be accurate for this range as well (see Table S3 in the ESI† for such predictions). A search using the results presented here for C_2H_3DO would be very promising for a first observation of an isotopically chiral molecule in space. It would reveal the D/H ratio for this molecule in the astrophysical environment. The accurate description of the observed spectra in our work is equally important for the future laboratory studies of rovibrational spectra of this isotopically chiral molecule. Our results may furthermore have implications for future studies of parity violation in isotopically chiral molecules.[49,50] Of course, even at the highest resolutions in our GHz and THz spectra, effects from parity violation are far too small to be detectable. However, the rovibrationally analysed spectra are the first step needed in the very special experiments designed to measure the small parity violating energy difference between the enantiomers of chiral molecules.[3,52]

Conflicts of interest

There are no conflicts to declare.

Acknowledgements

We enjoyed help and support from as well as discussions with Irina Bolotova, Hans Hollenstein, Carine Manca Tanner, Roberto Marquardt, Frédéric Merkt, Georg Seyfang and Jürgen Stohner. Our research is funded by ETH Zürich, in particular the Laboratory of Physical Chemistry, as well as a presidential grant, the Swiss National Science Foundation, an ERC Advanced Grant and the COST project MOLIM. K. K. thanks the Marie Heim-Vögtlin Program of the SNSF for financial support. The research leading to these results has in particular also received funding from the European Union's seventh Framework Program (FP7/2007-2013) ERC grant agreement no. 290925 [SPEQUACHIRAL2].

References

1 C. Ceccarelli, *Planet. Space Sci.*, 2002, **50**, 1267–1273.
2 E. Roueff and M. Gerin, *Space Sci. Rev.*, 2003, **106**, 61–72.
3 M. Quack, Fundamental Symmetries and Symmetry Violations from High-resolution Spectroscopy, in *Handbook of High Resolution Spectroscopy*, ed. M. Quack and F. Merkt, Wiley and Sons, Chichester, 2011, ch. 18, vol. 1, pp. 659–722.
4 M. Quack, *Angew. Chem.*, 1989, **101**, 588–604 (*Angew. Chem., Int. Ed.*, 1989, **28**, 571–586).
5 M. Quack, J. Stohner and M. Willeke, *Annu. Rev. Phys. Chem.*, 2008, **59**, 741–769.
6 J. E. Dickens, W. M. Irvine, M. Ohishi, M. Ikeda, S. Ishikawa, A. Nummelin and A. Hjalmarson, *Astrophys. J.*, 1997, **489**, 753–757.
7 A. Nummelin, J. E. Dickens, P. Bergman, A. Hjalmarson, W. M. Irvine, M. Ikeda and M. Ohishi, *Astron. Astrophys.*, 1998, **337**, 275–286.
8 M. Ikeda, M. Ohishi, A. Nummelin, J. E. Dickens, P. Bergman, A. Hjalmarson, W. M. Irvine and S. Ishikawa, *Astrophys. J.*, 2001, **560**, 792–805.
9 M. A. Requena-Torres, J. Martn-Pintado, S. Martn and M. R. Morris, *Astrophys. J.*, 2008, **672**, 352–360.
10 L. S. Bernstein and D. K. Lynch, *Astrophys. J.*, 2009, **704**, 226–239.
11 G. Cunningham Jr., A. W. Boyd, R. J. Myers, W. D. Gwinn and W. I. Le Van, *J. Chem. Phys.*, 1951, **19**, 676–685.
12 C. Hirose, *Bull. Chem. Soc. Jpn.*, 1974, **47**, 1311–1318.
13 R. A. Creswell and R. H. Schwendeman, *Chem. Phys. Lett.*, 1974, **27**, 521–524.
14 L. Pan, S. Albert, K. V. L. N. Sastry, E. Herbst and F. C. De Lucia, *Astrophys. J.*, 1998, **499**, 517–519.
15 D. T. Petkie, T. M. Goyette, R. P. A. Bettens, S. P. Belov, S. Albert, P. Helminger and F. C. De Lucia, *Rev. Sci. Instrum.*, 1997, **68**, 1675–1683.
16 C. Medcraft, C. D. Thompson, E. G. Robertson, D. R. T. Appadoo and D. McNaughton, *Astrophys. J.*, 2012, **753**, 18.
17 D. K. Russell and R. Wesendrup, *J. Mol. Spectrosc.*, 2003, **217**, 59–71.
18 W. J. Lafferty, J. M. Flaud, F. Kwabia Tchana and J. M. Fernandez, *Mol. Phys.*, 2013, **111**, 1983–1986.
19 J. M. Flaud, W. J. Lafferty, F. Kwabia Tchana, A. Perrin and X. Landsheere, *J. Mol. Spectrosc.*, 2012, **271**, 38–43.
20 F. Kwabia Tchana, M. Ngom, A. Perrin, J. M. Flaud, W. J. Lafferty, S. A. Ndiaye and El A. Ngom, *J. Mol. Spectrosc.*, 2013, **292**, 1–4.
21 F. Kwabia Tchana, J. M. Flaud, W. J. Lafferty and M. Ngom, *Mol. Phys.*, 2014, **112**, 1633–1638.
22 C. Puzzarini, M. Biczysko, J. Bloino and V. Barone, *Astrophys. J.*, 2014, **785**, 107.
23 H. Hollenstein, D. Luckhaus, J. Pochert, M. Quack and G. Seyfang, *Angew. Chem.*, 1997, **109**, 136–140 (*Angew. Chem., Int. Ed.*, 1997, **36**, 140–143).
24 R. Berger, M. Quack and J. Stohner, *Angew. Chem.*, 2001, **113**, 1716–1719 (*Angew. Chem., Int. Ed.*, 2001, **40**, 1667–1670).
25 K. K. Albert, S. Albert, M. Quack, J. Stohner, O. Trapp and V. Schurig, in Proceedings of the 19th Colloquium on High-Resolution Molecular Spectroscopy, Salamanca Spain, 2005, paper H15 and to be published.
26 S. Albert, Z. Chen, Ph. Lerch, K. Keppler, M. Quack, V. Schurig and O. Trapp, in Proceedings of the XXth Symposium of Atomic, Cluster and Surface Physics (SASP2016), Davos Switzerland, February 7–12, 2016, pp. 161–164, Innsbruck University Press, Innsbruck 2016 ISBN 978-903122-04-08.

27 S. Albert, Z. Chen, Ph. Lerch, K. Keppler, M. Quack, V. Schurig and O. Trapp, 72nd International Symposium on Molecular Spectroscopy, Urbana, IL, USA, June 17–21, paper WA01, 2017, DOI: 10.15278/isms.2017.WA01.

28 M. Suter and M. Quack, *Appl. Opt.*, 2015, **54**, 4417–4431.

29 S. Albert, I. Bolotova, Z. Chen, C. Fabri, L. Horny, M. Quack, G. Seyfang and D. Zindel, *Phys. Chem. Chem. Phys.*, 2016, **18**, 21976–21993.

30 S. Albert, F. Arn, I. Bolotova, Z. Chen, C. Fábri, G. Grassi, P. Lerch, M. Quack, G. Seyfang, A. Wokaun and D. Zindel, *J. Phys. Chem. Lett.*, 2016, **7**, 3847–3853.

31 S. Albert, Z. Chen, C. Fabri, Ph. Lerch, R. Prentner and M. Quack, *Mol. Phys.*, 2016, **114**, 2751–2768.

32 S. Albert, K. Keppler Albert, P. Lerch and M. Quack, *Faraday Discuss.*, 2011, **150**, 71–99.

33 S. Albert, S. Bauerecker, E. E. Bekhtereva, I. B. Bolotova, H. Hollenstein, M. Quack and O. N. Ulenikov, *Mol. Phys.*, 2018, **116**, 1091–1107.

34 S. Albert, K. Keppler Albert and M. Quack, High Resolution Fourier Transform Infrared Spectroscopy, in *Handbook of High Resolution Spectroscopy*, ed. M. Quack and F. Merkt, Wiley, Ltd, 2011, ch. 26, vol. 2, pp. 965–1019.

35 S. Albert, K. Keppler, P. Lerch, M. Quack and A. Wokaun, *J. Mol. Spectrosc.*, 2015, **315**, 92–101.

36 L. S. Rothman, I. E. Gordon, A. Barbe, D. Chris Benner, P. F. Bernath, M. Birk, V. Boudon, L. R. Brown, A. Campargue, J.-P. Champion, K. Chance, L. H. Coudert, V. Danaj, V. M. Devi, S. Fally, J.-M. Flaud, R. R. Gamache, A. Goldmann, D. Jacquemart, I. Kleiner, N. Lacome, W. J. Lafferty, J.-Y. Mandin, S. T. Massie, S. N. Mikhailenko, C. E. Miller, N. Moazzen-Ahmadi, O. V. Naumenko, A. V. Nikitin, J. Orphal, V. I. Perevalov, A. Perrin, A. Predoi-Cross, C. P. Rinsland, M. Rotger, M. Šimecková, M. A. H. Smith, K. Sung, S. A. Tashkun, J. Tennyson, R. A. Toth, A. C. Vandaele and J. Vander Auwera, *J. Quant. Spectrosc. Radiat. Transfer*, 2009, **110**, 533.

37 J. K. G. Watson, in *Vibrational Spectra and Structure*, ed. J. Durig, Elsevier, Amsterdam, 1977, vol. 6, pp. 1–89.

38 S. Albert, K. Keppler Albert, H. Hollenstein, C. Manca Tanner and M. Quack, Fundamentals of Rotation-Vibration Spectra, in *Handbook of High Resolution Spectroscopy*, ed. M. Quack and F. Merkt, Wiley, Ltd, 2011, ch. 3, vol. 2, pp. 117–173.

39 D. Luckhaus and M. Quack, *Mol. Phys.*, 1989, **68**, 745–758.

40 R. Signorell, R. Marquardt, M. Quack and M. A. Suhm, *Mol. Phys.*, 1996, **89**, 297–313.

41 H. Hollenstein, R. Marquardt, M. Quack and M. A. Suhm, *J. Chem. Phys.*, 1994, **101**, 3588–3602.

42 H. Hollenstein, R. Marquardt, M. Quack and M. A. Suhm, *Ber. Bunsenges. Phys. Chem.*, 1995, **99**, 275–281.

43 S. Albert and M. Quack, *ChemPhysChem*, 2007, **8**, 1271–1281.

44 A. Bauder, Fundamentals of Rotational Spectroscopy, in *Handbook of High Resolution Spectroscopy*, ed. M. Quack and F. Merkt, Wiley, John Wiley & Sons, Ltd, 2011, ch. 2, vol. 1, pp. 57–116.

45 C. M. Western, *PGOPHER version 9.1*, University of Bristol Research Data Repository, 2016, DOI: 10.5523/bris.1nz94wvrfzzdo1d67et0t4v4nc.

46 C. M. Western, Introduction to Modeling High-resolution Spectra, in *Handbook of High Resolution Spectroscopy*, ed. M. Quack and F. Merkt, Wiley, John Wiley & Sons, Ltd, 2011, ch. 1, vol. 3, pp. 1415–1435.

47 F. Tullini, G. D. Nivellini and M. Carlotti, *J. Mol. Spectrosc.*, 1989, **138**, 355–374 and literature cited therein.

48 J. M. Lykke, A. Coutens, J. K. Jørgensen, M. H. D. van der Wiel, R. T. Garrod, H. S. P. Müller, P. Bjerkeli, T. L. Bourke, H. Calcutt, M. N. Drozdovskaya, C. Favre, E. C. Fayolle, S. K. Jacobsen, K. I. Öberg, M. V. Persson, E. F. van Dishoeck and S. F. Wampfler, *Astron. Astrophys.*, 2017, **597**, A53.

49 R. Berger, M. Quack, A. Sieben and M. Willeke, *Helv. Chim. Acta*, 2003, **86**, 4048–4060.

50 R. Berger, G. Laubender, M. Quack, A. Sieben, J. Stohner and M. Willeke, *Angew. Chem.*, 2005, **117**, 3689–3693 (*Angew. Chem., Int. Ed.*, 2005, **44**, 3623–3626).

51 H. C. Longuet-Higgins, *Mol. Phys.*, 1963, **6**(5), 445–460.

52 P. Dietiker, E. Miloglyadov, M. Quack, A. Schneider and G. Seyfang, *J. Chem. Phys.*, 2015, **143**, 244305.